

**Water vapor
transport in the lower
mesosphere**

T. Flury et al.

Water vapor transport in the lower mesosphere of the subtropics: a trajectory analysis

T. Flury, S. C. Müller, K. Hocke, and N. Kämpfer

Institute of Applied Physics, University of Bern, Sidlerstrasse 5, 3012 Bern, Switzerland

Received: 10 June 2008 – Accepted: 23 June 2008 – Published: 18 July 2008

Correspondence to: T. Flury (thomas.flury@iap.unibe.ch)

Published by Copernicus Publications on behalf of the European Geosciences Union.

Title Page

Abstract

Introduction

Conclusions

References

Tables

Figures

◀

▶

◀

▶

Back

Close

Full Screen / Esc

Printer-friendly Version

Interactive Discussion



Abstract

The Institute of Applied Physics operates an airborne microwave radiometer that measures the rotational transition line of water vapor at 183.3 GHz. Measurements were acquired on board a Learjet once a year in the period 1998 to 2006. Water vapor profiles are retrieved for the altitude range from 15 to 75 km along the flight track. We report on a water vapor enhancement in the lower mesosphere above India and the Arabic Sea measured on our flight mission in November 2005 conducted during EC-project SCOUT-O3. The flight led from Switzerland to Australia and back. We find an enhancement of up to 25% in the lower mesospheric H₂O volume mixing ratio measured on the return flight one week after the outward flight. The origin of the air is traced back by means of a trajectory model in the lower mesosphere. During the outward flight the air came from the Caribbean and crossed the Atlantic Ocean. On the return flight the air came from China and originated from mid latitudes. Thus the large variability of H₂O VMR during our flight is explained by a change of the winds in the lower mesosphere.

1 Introduction

Water vapor plays a key role in atmospheric processes. In the troposphere it acts as a strong greenhouse gas and is responsible for the weather mechanisms such as convection, cloud formation and latent heat release. In the stratosphere H₂O contributes to radiative cooling and plays a role in ozone depletion chemistry by the formation of polar stratospheric clouds. In the lower mesosphere as well as in the stratosphere water vapor can be used as a tracer for atmospheric transport. Further it is involved in the buildup of polar mesospheric clouds also known as noctilucent clouds at the mesopause. Finally water vapor is dissociated by photolysis in the upper mesosphere inducing catalytic destruction of odd oxygen. The H₂O volume mixing ratio (VMR) decreases from a few percent in the tropical troposphere to a few parts per million in the

ACPD

8, 13775–13799, 2008

Water vapor transport in the lower mesosphere

T. Flury et al.

Title Page

Abstract

Introduction

Conclusions

References

Tables

Figures

◀

▶

◀

▶

Back

Close

Full Screen / Esc

Printer-friendly Version

Interactive Discussion



mesosphere. The measurement over 4 orders of magnitude is difficult to be achieved by one single measurement technique. We use ground-based and airborne microwave remote sensing for the retrieval of H₂O VMR in the middle atmosphere (Deuber et al., 2005; Müller et al., 2008). A typical water vapor profile measured by our airborne microwave radiometer AMSOS is shown in Fig. 1: H₂O VMR decreases exponentially in the troposphere to reach a minimum at the so called hygropause which is slightly above the tropopause. In the stratosphere H₂O VMR increases again due to oxidation of methane and reaches a maximum at the stratopause and lower mesosphere. The chemical lifetime of water vapor in the middle atmosphere is of the order of years in the lower stratosphere and months in the lower mesosphere (Brasseur and Solomon, 2005), allowing for water vapor to be used as a tracer in the upper stratosphere and lower mesosphere. Atmospheric circulation models show a strong zonal wind prevailing in the lower mesosphere (50 to 70 km altitude) and changing its direction around equinox. The wind is in an eastward direction in the winter hemisphere and westward in the summer hemisphere. Zonal-mean zonal wind of the CIRA86 climatology (Fleming et al., 1990) for November is given in Fig. 2. Eastward and westward wind in the middle atmosphere are a consequence of the pole to pole circulation which is mainly due to latitudinal temperature differences and to gravity wave breaking at the mesopause, which decelerates the zonal flow by the deposition of angular momentum. The change of the zonal flow induces a meridional transport according to the conservation of angular momentum (Shepherd, 2000). Solar Lyman- α flux determines the photolysis of water vapor in the middle atmosphere. The latitude-dependent radiation budget leads to a mesospheric H₂O VMR gradient from equator to pole as the radiation is more intense at the equator, thus mesospheric meridional transport affects the H₂O VMR distribution.

Water vapor transport in the lower mesosphereT. Flury et al.

[Title Page](#)[Abstract](#)[Introduction](#)[Conclusions](#)[References](#)[Tables](#)[Figures](#)[⏪](#)[⏩](#)[◀](#)[▶](#)[Back](#)[Close](#)[Full Screen / Esc](#)[Printer-friendly Version](#)[Interactive Discussion](#)

2 Instrument

AMSOS (Airborne Microwave Stratospheric Observing System) is a total-power radiometer based on a conventional uncooled heterodyne receiver using a Schottky diode mixer as reported by Vasic et al. (2005). The instrument measures the thermal emission of the pressure broadened water vapor rotational transition line at 183.3 GHz, which allows the retrieval of H₂O altitude profiles. Two digital Fast Fourier Transform spectrometers resolve the spectral line with a channel resolution of 61 kHz and 12 kHz Müller et al. (2008)¹. The main result of AMSOS are water vapor profiles between 15 and 75 km from polar regions to the tropics as reported by Feist et al. (2007) and Müller et al. (2008). AMSOS is flown on board a Swiss Airforce Learjet and was operated once a year since 1998. The line of sight of the instrument is perpendicular to the flight direction with an elevation angle of 20 degrees. Such a geometry facilitates the data analysis for the wind retrieval which is another product of AMSOS as reported by Flury et al. (2008)².

3 Measurements and data analysis

AMSOS measures continuously during flights with a horizontal resolution of 30 to 100 km depending on the integration time of the spectrometers and the measurement noise. The vertical resolution is between 10 and 15 km for the upper stratosphere and lower mesosphere (Müller et al., 2008). Narrowband spectrometers with a high channel resolution allow a retrieval of water vapor for mesospheric altitudes while broadband spectrometers are able to provide information about the upper troposphere and lower

¹Müller, S. C., Murk, A., Monstein, C., and Kämpfer, N.: Intercomparison of Digital Fast Fourier Transform and Accousto Optical spectrometers for microwave radiometry of the atmosphere, IEEE T. Geosci. Remote, in review, 2008.

²Flury, T., Hocke, K., Müller, S., and Kämpfer, N.: First measurements of lower mesospheric wind by airborne microwave radiometry, Geophys. Res. Lett., in review, 2008.

Water vapor transport in the lower mesosphere

T. Flury et al.

Title Page

Abstract

Introduction

Conclusions

References

Tables

Figures



Back

Close

Full Screen / Esc

Printer-friendly Version

Interactive Discussion



stratosphere. This fact is due to the analysis of the pressure broadened line: The better the line center is resolved the more information one gets about the mesosphere whilst the broader the spectrum is the more information one gets out of the wings of the spectrum, which are assigned to the lower part of the middle atmosphere. This work focusses on the narrowband FFT spectrometer which gives access to the altitude range from 45 to 75 km.

Water vapor profiles are retrieved by an optimal estimation method (Rodgers, 2000) which is implemented in the inversion software package ARTS/QPack (Buehler et al., 2005; Eriksson et al., 2005).

4 Results and discussion

A total of 300 mesospheric profiles were retrieved for the SCOUT-O3 flight campaign along the flight track shown in Fig. 3. Figure 4 shows all the H₂O profiles time ordered for the outward and return flight. The flight route was chosen identically for both flights. H₂O VMR is between 2 and 8 ppm. A mesospheric latitudinal gradient is clearly visible above 65 km during the outward flight where the ratio drops from values of about 6.5 ppm north of 30° N to 5 ppm south of it. This is possibly explained by the so called tropical pipe model, with dynamical barriers between low and middle latitudes, (Plumb, 1996). There is a significant difference between the outward and return flight above the Arabic Sea and India, marked by two rectangles in Fig. 4, which starts at 60° E and 23° N and ends at 70° E and 20° N and also between the first and last part of the flight over the Mediterranean Sea highlighted by two ellipses. AMSOS measured between 15% and 25% more water vapor above 55 km on the return flight over India one week after the outward flight on 8 November 2005 which is shown in Fig. 5 whereas AMSOS measured up to 25% less at same altitudes on the return flight over the Mediterranean, see Fig. 6.

A mesospheric water vapor enhancement of this extent must be due to transport of airmasses from regions of higher H₂O VMR. As there are no strong sources of wa-

Water vapor transport in the lower mesosphere

T. Flury et al.

Title Page

Abstract

Introduction

Conclusions

References

Tables

Figures

◀

▶

◀

▶

Back

Close

Full Screen / Esc

Printer-friendly Version

Interactive Discussion



ter vapor in the lower mesosphere, analysis of horizontal air parcel trajectories may solve the mystery of the enhancement. Normally we use the Goddard Automailer trajectory model (http://code916.gsfc.nasa.gov/Data_services/automailer/index.html), but unfortunately it does not provide mesospheric trajectories based on ECMWF wind data which are possibly the best estimates for this altitude region. ECMWF wind fields are available up to an altitude of 65 km in November 2005. By means of a simple trajectory model TomTOM (Tom's Trajectory Model), developed by one of the authors, we calculate trajectories. The model is set up in a Matlab code and interpolates directly ECMWF wind data on the exact air parcel location. ECMWF values, which are spread on a 1.125° grid are stored in our Institute's MySQL database with user-friendly search options. Matlab accesses directly these data and calculates trajectories on isentropes since air parcels move on levels of constant potential temperature. Matlab provides the trajectory datafile and a geographic map with the trajectory as output. A flow chart of TomTOM is sketched in Fig. 7.

4.5 days backward trajectories were calculated for both flight tracks of outward and return flight over the Arabic Sea. The outward flight took place on 8 November and the return flight one week later on 15 November. Consequently air parcel trajectories were calculated back to the starting days 4th and 11th of November for the 2700 K isentropic surface which corresponds approximately to an altitude of 60 km. The results are shown in Figs. 8 and 9. There is in fact a huge difference in the trajectories as there is one in H_2O VMR. For the outward flight air parcels came in an eastward current across the Atlantic Ocean whilst one week later the wind direction changed and parcels moved on a southward-westward current and started mainly over China. This change in trajectories shows the strong dynamical variability of the lower mesosphere over India where a reversal of the zonal wind direction occurred. A look at a measured global lower mesospheric water vapor map of the Aura/MLS satellite experiment (<http://mls.jpl.nasa.gov/data/gallery.php>) confirms that there was about 20% less water vapor in the region of the Caribbean Sea on 4 November, where the air parcels started, compared to one week later over China. This can be seen in the MLS maps in Fig. 10 for 4

**Water vapor
transport in the lower
mesosphere**T. Flury et al.

Title Page

Abstract

Introduction

Conclusions

References

Tables

Figures

◀

▶

◀

▶

Back

Close

Full Screen / Esc

Printer-friendly Version

Interactive Discussion



November and Fig. 11 for 11 November. Relatively dry air masses were transported to India from tropical regions near Jamaica during the outward flight, whereas one week later more humid air from middle and high latitudes was transported into the same region passing over China.

5 A similar difference in lower mesospheric water vapor was also measured over the Mediterranean. Figure 6 shows that there was about 20% more water vapor during the outward flight on 4 November than during the return flight on 16 November. The same trajectory analysis is done for this situation. 3 days backward trajectories were calculated along the flighttrack on the 2600 K isentrope, which corresponds approximately
10 to 58 km. Results are shown in Figs. 12 and 13. There is a considerable difference in the first part of the trajectories: for the return flight Fig. 13, air parcels moved first northward entered the US around 40° N turned again southward and crossed the Atlantic Ocean similar to the air parcels calculated for the outward flight in Fig. 14. During the outward flight air parcels moved between 22° N and 30° N, which is 10° more south
15 than 12 days later, crossed Florida and the Atlantic Ocean. The sinusoidal structure of the trajectories in Fig. 13 is probably due to a planetary wave. A look on the Aura/MLS water vapor measurements reveals that there is a significant difference in mesospheric H₂O VMR over the west coast of Mexico on 1 November and the west coast of the US around 40° N on 13 November where the air parcels passed through. Air parcels
20 for the outward flight crossed Mexico in a region of about 6.4 ppm H₂O as visible in Fig. 14, whilst 12 days later around 40° N on the East-coast of the US volume mixing ratios of about 5.5 ppm are found see Fig. 15. This is a difference of approximately 16% and explains qualitatively the observed variation of H₂O VMR between both flight tracks over the Mediterranean Sea.

25 Currently studies for lower mesospheric transport are rare and the H₂O radiometers AMSOS and MIAWARA (Deuber et al., 2005) operated by our Institute of Applied Physics in Bern (Switzerland) provide useful information about dynamical processes in the lower mesosphere. This is an important issue as dynamics directly affects chemistry of the middle atmosphere and vice versa (Sonnemann and Grygalashvily, 2003).

Water vapor transport in the lower mesosphere

T. Flury et al.

Title Page

Abstract

Introduction

Conclusions

References

Tables

Figures

⏪

⏩

◀

▶

Back

Close

Full Screen / Esc

Printer-friendly Version

Interactive Discussion



5 Conclusions

This study is an example of how water vapor can be used as a tracer for lower mesospheric air mass transport. The measured water vapor enhancement over the Arabic Sea and India on the return flight was due to air mass transport from a different region. The change in air parcel trajectories is due to the changing zonal wind direction which is around 20° N latitude in November 2005. During the outward flight the mesospheric wind direction was eastward over Northern India whilst one week later it was already westward. The enhancement of up to 25% as measured by AMSOS is confirmed by Aura/MLS measurements as well as the difference in volume mixing ratio of the two different regions of origin of the air parcels namely the Caribbean and China, where air parcels started. The measured decrease in the section of the flight over the Mediterranean is also due to transport of air from different regions. The relatively dry air measured on the return flight passed through a dry region on the west coast of the United States. The different trajectories shown in Figs. 12 and 13 are probably due to a travelling planetary wave in this region. Finally microwave remote sensing has proven to be suitable for the study of atmospheric dynamics and composition changes. Presently it is not much known about transport processes in the lower mesosphere. With the extension of the upper boundary of the ECMWF reanalysis model, calculation of realistic trajectories is possible, which we find in agreement with AMSOS and Aura/MLS observations of the variability of lower mesospheric water vapor. Recent studies by Hoppel et al. (2008) and Berger (2008) also show the progress which has been achieved in data assimilation and modeling of the middle atmosphere.

Acknowledgements. This work has been supported by the EC-project SCOUT-O3 under grant SBF Nr. 03.0352-2 and by the Swiss National Science Foundation under grant Nr. 200020-115882/1. Thanks to the pilots of the Swiss Airforce Learjet and to Gloria Manney for the Aura/MLS global maps.

ACPD

8, 13775–13799, 2008

Water vapor transport in the lower mesosphere

T. Flury et al.

Title Page

Abstract

Introduction

Conclusions

References

Tables

Figures

◀

▶

◀

▶

Back

Close

Full Screen / Esc

Printer-friendly Version

Interactive Discussion



References

- Berger, U.: Modeling of middle atmosphere dynamics with LIMA, *J. Atmos. Solar Terr. Phys.*, 70, 8–9, 1170–1200, doi:10.1016/j.jastp.2008.02.004, June 2008. [13782](#)
- Brasseur, G. P. and Solomon, S.: *Aeronomy of the Middle Atmosphere Chemistry and Physics of the Stratosphere and Mesosphere Series: Atmospheric and Oceanographic Sciences Library*, vol. 32, 3rd rev. and enlarged ed., XII, 646 pp., Hardcover, ISBN: 978-1-4020-3284-4, 2005. [13777](#)
- Buehler, S., Eriksson, P., Kuhn, T., von Engel, A., and Verdes, C.: ARTS, the Atmospheric Radiative Transfer Simulator, *J. Quant. Spectrosc. Ra.*, 91, 65–93, 2005. [13779](#)
- Deuber, B., Haeefe, A., Feist, D. G., Martin, L., Kampfer, N., Nedoluha, G. E., Yushkov, V., Khaykin, S., Kivi, R., and Vömel, H.: Middle Atmospheric Water Vapour Radiometer – MI-AWARA: Validation and first results of the LAUTLOS/WAVVAP campaign, *J. Geophys. Res.*, 110, D13306, doi:10.1029/2004JD005543, 2005. [13777](#), [13781](#)
- Eriksson, P., Jimenés, C., and Buehler, S. A.: Qpack, a general tool for instrument simulation and retrieval work, *J. Quant. Spectrosc. Ra.*, 91, 47–64, doi:10.1016/j.jqsrt.2004.05.050, 2005. [13779](#)
- Feist, D. G., Geer, A. J., Müller, S., and Kämpfer, N.: Middle atmosphere water vapour and dynamical features in aircraft measurements and ECMWF analyses, *Atmos. Chem. Phys.*, 7, 5291–5307, 2007, <http://www.atmos-chem-phys.net/7/5291/2007/>. [13778](#)
- Fleming, E. L., Chandra, S., Barnett J. J., and Corney, M.: Zonal mean temperature, pressure, zonal wind and geopotential height as functions of latitude, *Adv. Space Res.*, 10, 12, 11–59, doi:10.1016/0273-1177(90)90383-E, 1990. [13777](#)
- Hoppel, K. W., Baker, N. L., Coy, L., Eckermann, S. D., McCormack, J. P., Nedoluha, G. E., and Siskind, D. E.: Assimilation of stratospheric and mesospheric temperatures from MLS and SABER into a global NWP model, *Atmos. Chem. Phys. Discuss.*, 8, 8455–8490, 2008, <http://www.atmos-chem-phys-discuss.net/8/8455/2008/>. [13782](#)
- Müller, S., Kämpfer, N., Feist, D., Haeefe, A., Milz, M., Sitnikov, N., Schiller, C., Kiemle, C., and Urban, J.: Validation of stratospheric water vapour measurements from the airborne microwave radiometer AMSOS, *Atmos. Chem. Phys.*, 8, 3169–3183, 2008, <http://www.atmos-chem-phys.net/8/3169/2008/>. [13777](#), [13778](#)
- Plumb, R. A.: A “tropical pipe” model of stratospheric transport, *J. Geophys. Res.*, 101, 3957–3972, doi:10.1029/95JD03002, 1996. [13779](#)

Water vapor transport in the lower mesosphere

T. Flury et al.

Title Page

Abstract

Introduction

Conclusions

References

Tables

Figures

◀

▶

◀

▶

Back

Close

Full Screen / Esc

Printer-friendly Version

Interactive Discussion



Rodgers, C. D.: Inverse Methods for Atmospheric Sounding: Theory and Practice, vol. 2 of Series on atmospheric, oceanic and planetary physics, World Scientific Publishing Co. Pte. Ltd., P.O. Box 128, Farrer Road, Singapore 912805, 2000. [13779](#)

5 Shepherd, T. G.: The middle atmosphere, J. Atmos. Sol.-Terr. Phy., 62, 1587–1601, 2000. [13777](#)

Sonnemann, G. R. and Grygalashvily, M.: The zonal wind effect on the photochemistry within the mesosphere/mesopause region, Adv. Space Res., 32, 719–724, doi:10.1016/S0273-1177(03)00406-X, 2003. [13781](#)

10 Vasic, V., Feist, D. G., Müller, S., and Kämpfer, N.: An airborne radiometer for stratospheric water vapor measurements at 183 GHz, IEEE T. Geosci. Remote, 43, 1563–1570, doi:10.1109/TGRS.2005.846860, 2005. [13778](#)

ACPD

8, 13775–13799, 2008

Water vapor transport in the lower mesosphere

T. Flury et al.

Title Page

Abstract

Introduction

Conclusions

References

Tables

Figures

◀

▶

◀

▶

Back

Close

Full Screen / Esc

Printer-friendly Version

Interactive Discussion



**Water vapor
transport in the lower
mesosphere**

T. Flury et al.

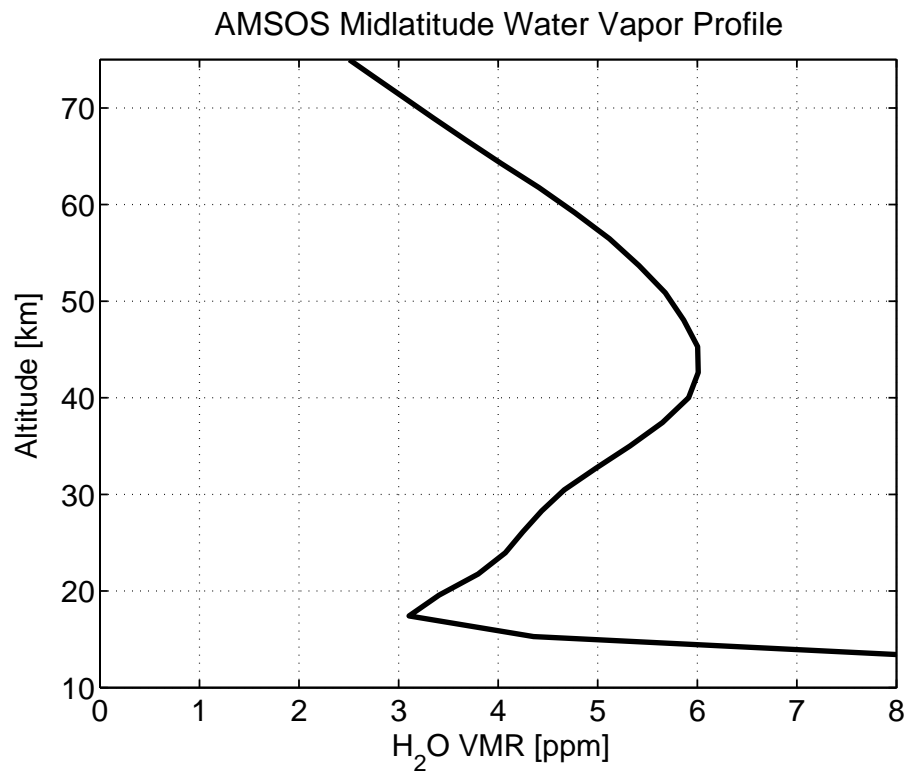


Fig. 1. A measured AMSOS midlatitude water vapor profile in November with the typical dry hygro-pause at 18 km and a middle atmospheric local maximum around the stratopause at 45 km.

[Title Page](#)[Abstract](#)[Introduction](#)[Conclusions](#)[References](#)[Tables](#)[Figures](#)[◀](#)[▶](#)[◀](#)[▶](#)[Back](#)[Close](#)[Full Screen / Esc](#)[Printer-friendly Version](#)[Interactive Discussion](#)

**Water vapor
transport in the lower
mesosphere**

T. Flury et al.

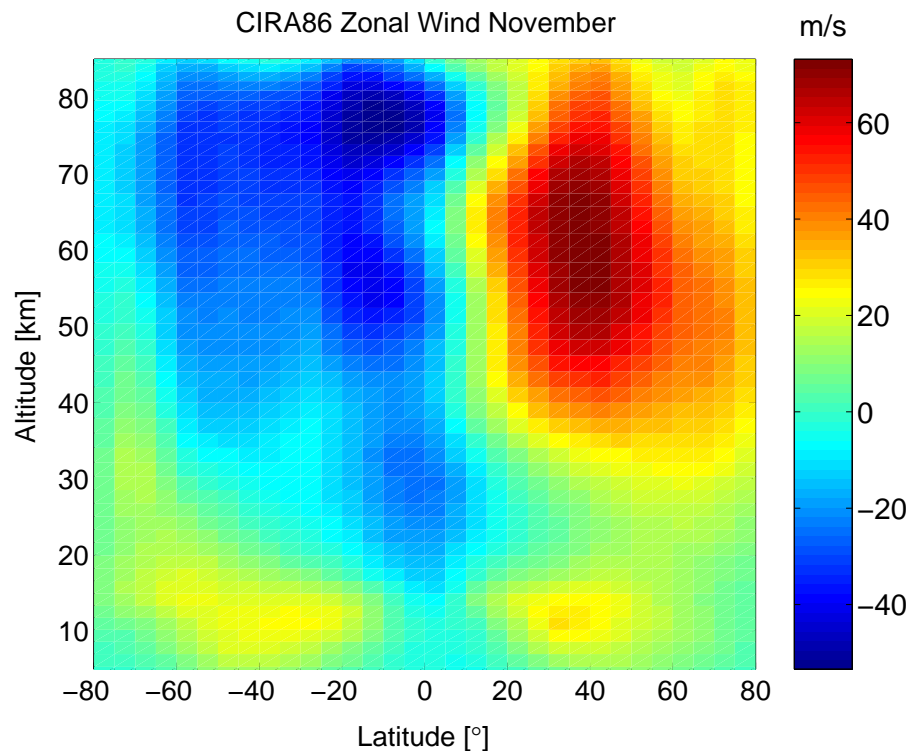


Fig. 2. CIRA 86 climatology for the zonal mean zonal wind. The Southern- and Northern Hemisphere tropopause jet stream can be seen at 12 km as well as the different wind directions in the middle atmosphere: Eastward in winter, westward in summer.

[Title Page](#)[Abstract](#)[Introduction](#)[Conclusions](#)[References](#)[Tables](#)[Figures](#)[◀](#)[▶](#)[◀](#)[▶](#)[Back](#)[Close](#)[Full Screen / Esc](#)[Printer-friendly Version](#)[Interactive Discussion](#)

**Water vapor
transport in the lower
mesosphere**T. Flury et al.

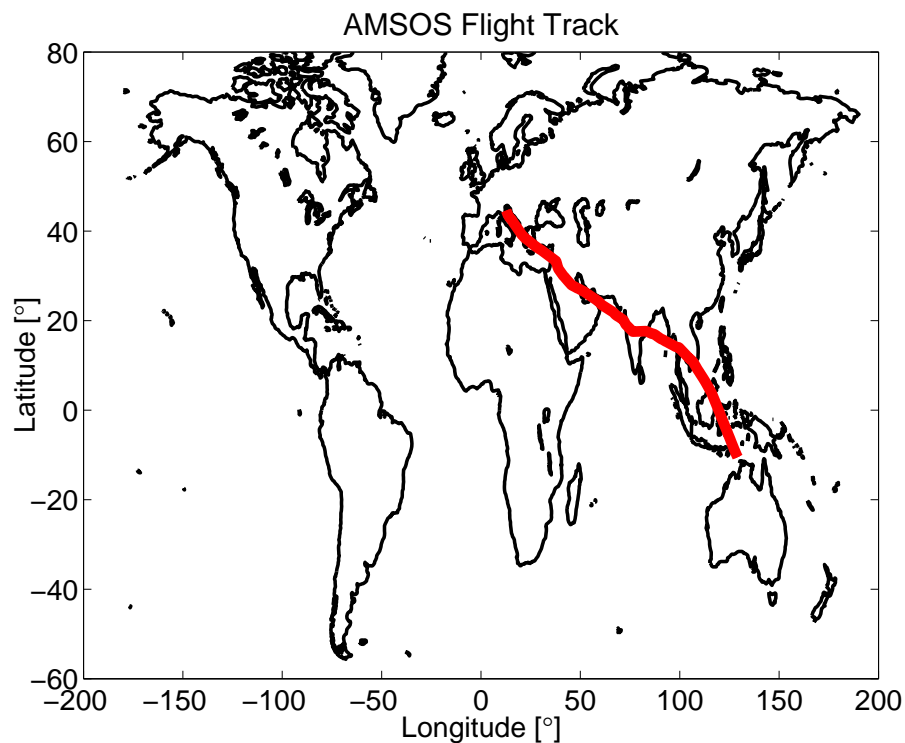


Fig. 3. AMSOS flight track for the SCOUT-O3 campaign transfer flight in November 2005.

[Title Page](#)[Abstract](#)[Introduction](#)[Conclusions](#)[References](#)[Tables](#)[Figures](#)[◀](#)[▶](#)[◀](#)[▶](#)[Back](#)[Close](#)[Full Screen / Esc](#)[Printer-friendly Version](#)[Interactive Discussion](#)

Water vapor transport in the lower mesosphere

T. Flury et al.

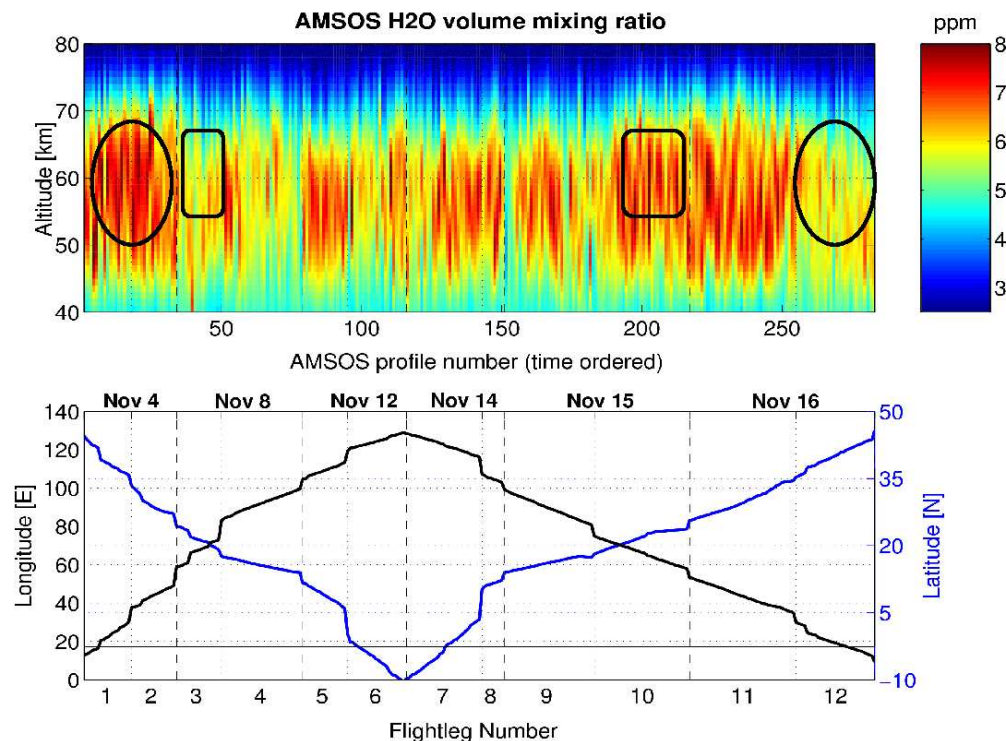


Fig. 4. Retrieved water vapor profiles ordered in time and the corresponding location given in longitude and latitude below. The water vapor maximum is around 60 km altitude in the extratropics and lower in the tropics, where it is around 55 km. Vertically fine dotted lines represent fuel stops on a same day and vertically dashed lines represent stops for one or several days. The two ellipses and rectangles highlight the significant differences on the outward and return flight. The ellipsis covers the Mediterranean profiles whilst the rectangle covers the situation above India.

Title Page

Abstract

Introduction

Conclusions

References

Tables

Figures

◀

▶

◀

▶

Back

Close

Full Screen / Esc

Printer-friendly Version

Interactive Discussion



**Water vapor
transport in the lower
mesosphere**

T. Flury et al.

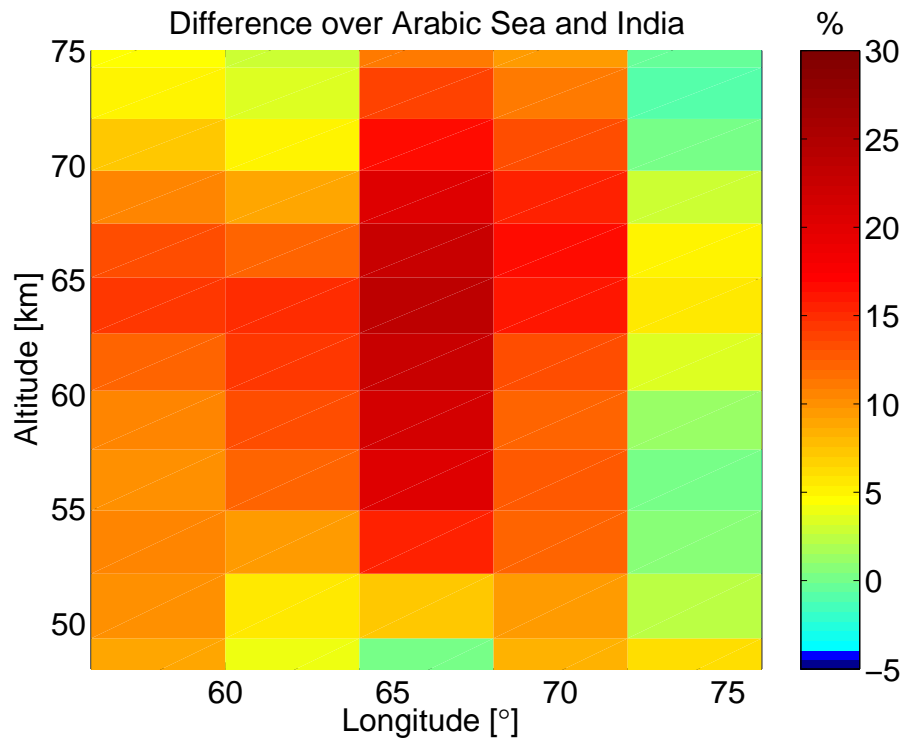


Fig. 5. The relative difference of return and outward flight H_2O VMR over the Arabic Sea and India in the lower mesosphere. AMSOS measured up to 25% more water vapor on the return flight.

[Title Page](#)[Abstract](#)[Introduction](#)[Conclusions](#)[References](#)[Tables](#)[Figures](#)[◀](#)[▶](#)[◀](#)[▶](#)[Back](#)[Close](#)[Full Screen / Esc](#)[Printer-friendly Version](#)[Interactive Discussion](#)

**Water vapor
transport in the lower
mesosphere**

T. Flury et al.

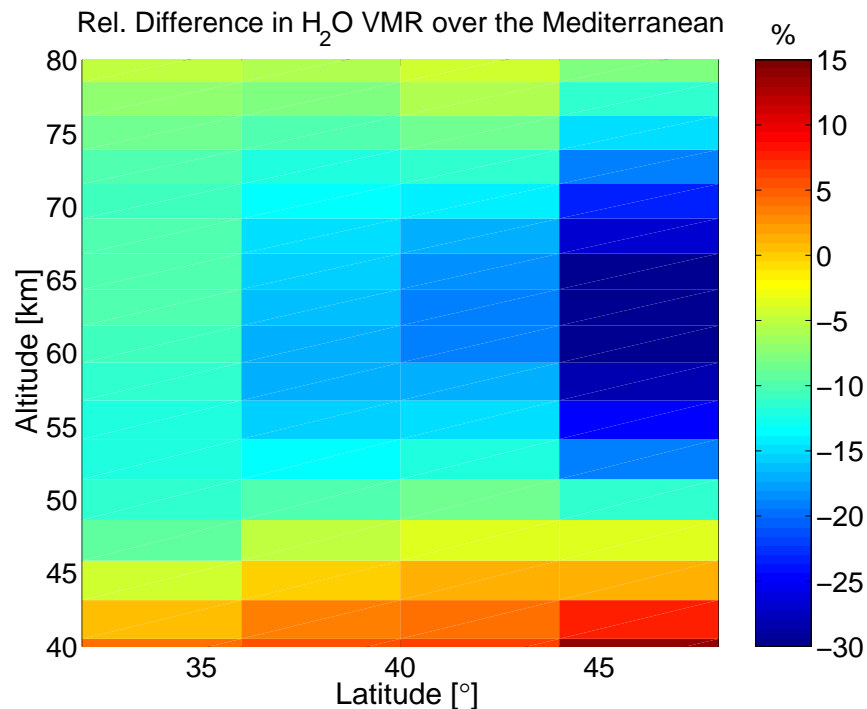


Fig. 6. The relative difference of return and outward flight in H₂O VMR over the Mediterranean Sea in the lower mesosphere. There were 2 weeks between both measurements in November 2005. AMSOS measured up to 25% less water vapor on the return flight.

[Title Page](#)[Abstract](#)[Introduction](#)[Conclusions](#)[References](#)[Tables](#)[Figures](#)[◀](#)[▶](#)[◀](#)[▶](#)[Back](#)[Close](#)[Full Screen / Esc](#)[Printer-friendly Version](#)[Interactive Discussion](#)

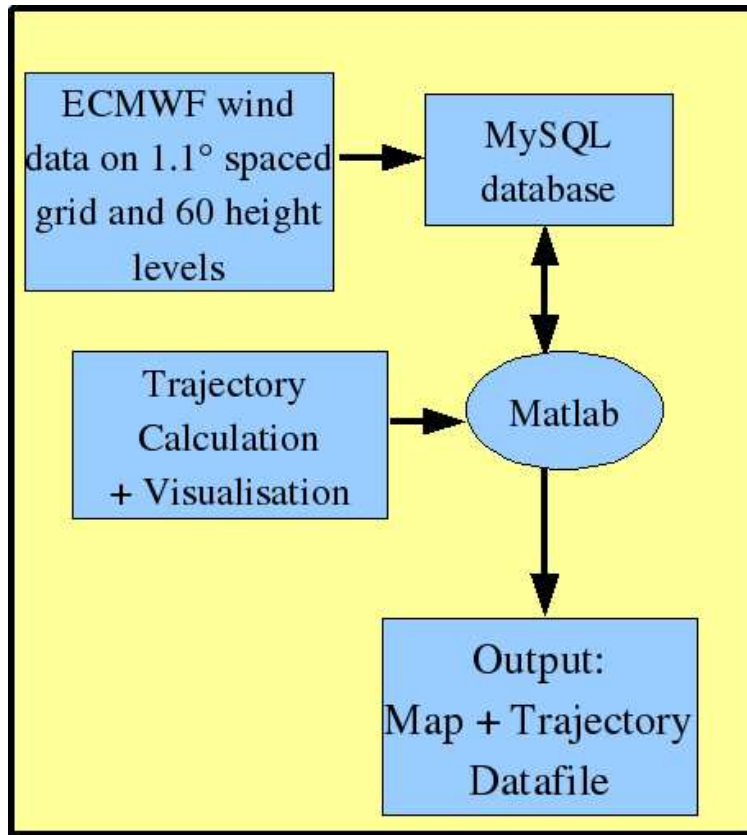


Fig. 7. Tom's Trajectory Model TomTOM based on ECMWF wind data. Trajectory calculation is implemented in a Matlab routine which takes directly the corresponding ECMWF wind data using the institute's MySQL database.

Water vapor transport in the lower mesosphere

T. Flury et al.

Title Page

Abstract Introduction

Conclusions References

Tables Figures

◀ ▶

◀ ▶

Back Close

Full Screen / Esc

Printer-friendly Version

Interactive Discussion



**Water vapor
transport in the lower
mesosphere**

T. Flury et al.

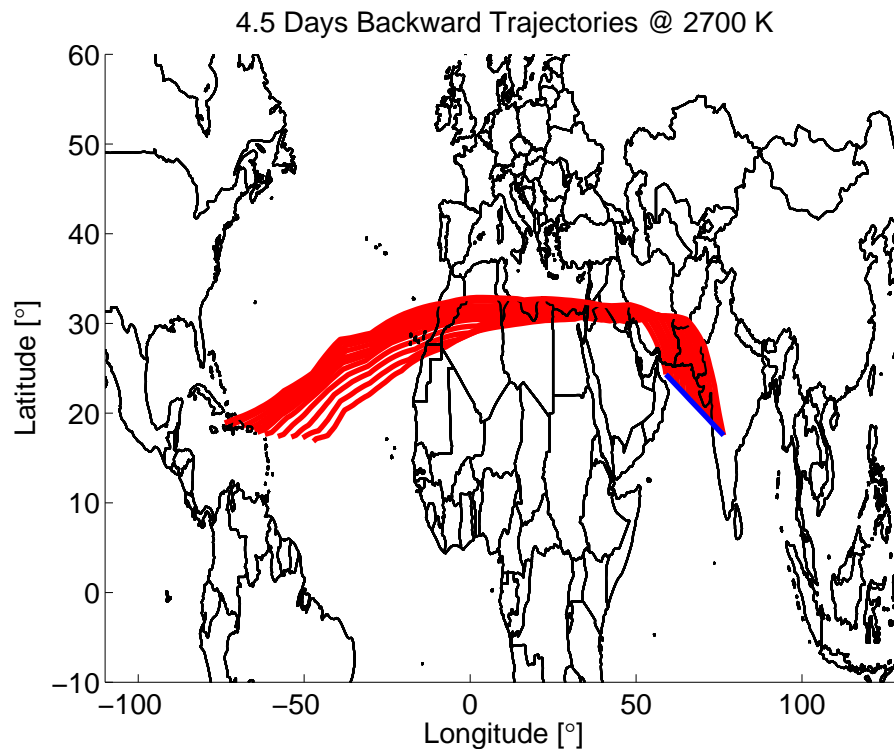


Fig. 8. Backward trajectories along the outward flight calculated on the 2700 K isentropes. The blue line indicates the flight track from west to east. Parcels start on 4 November over the Caribbean Sea and reach the blue flight track on 8 November.

[Title Page](#)[Abstract](#)[Introduction](#)[Conclusions](#)[References](#)[Tables](#)[Figures](#)[◀](#)[▶](#)[◀](#)[▶](#)[Back](#)[Close](#)[Full Screen / Esc](#)[Printer-friendly Version](#)[Interactive Discussion](#)

**Water vapor
transport in the lower
mesosphere**

T. Flury et al.

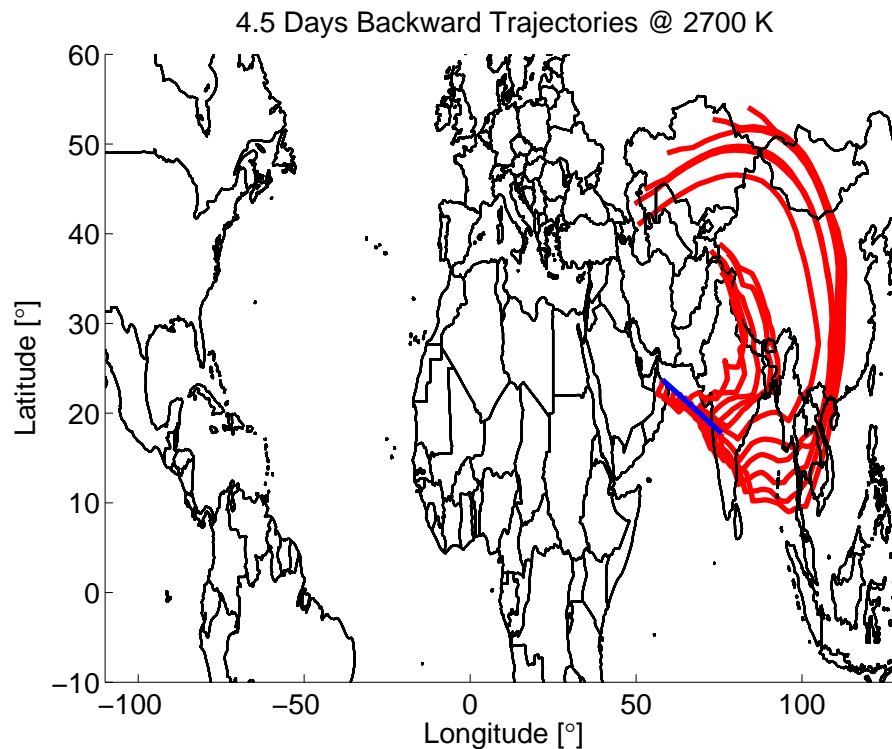


Fig. 9. Backward trajectories along the return flight calculated on the 2700 K isentropes. The blue line indicates the flight track east to west. Parcels start on 11 November over central Asia and China and reach the blue flight track on 15 November.

[Title Page](#)[Abstract](#)[Introduction](#)[Conclusions](#)[References](#)[Tables](#)[Figures](#)[◀](#)[▶](#)[◀](#)[▶](#)[Back](#)[Close](#)[Full Screen / Esc](#)[Printer-friendly Version](#)[Interactive Discussion](#)

Water vapor transport in the lower mesosphere

T. Flury et al.

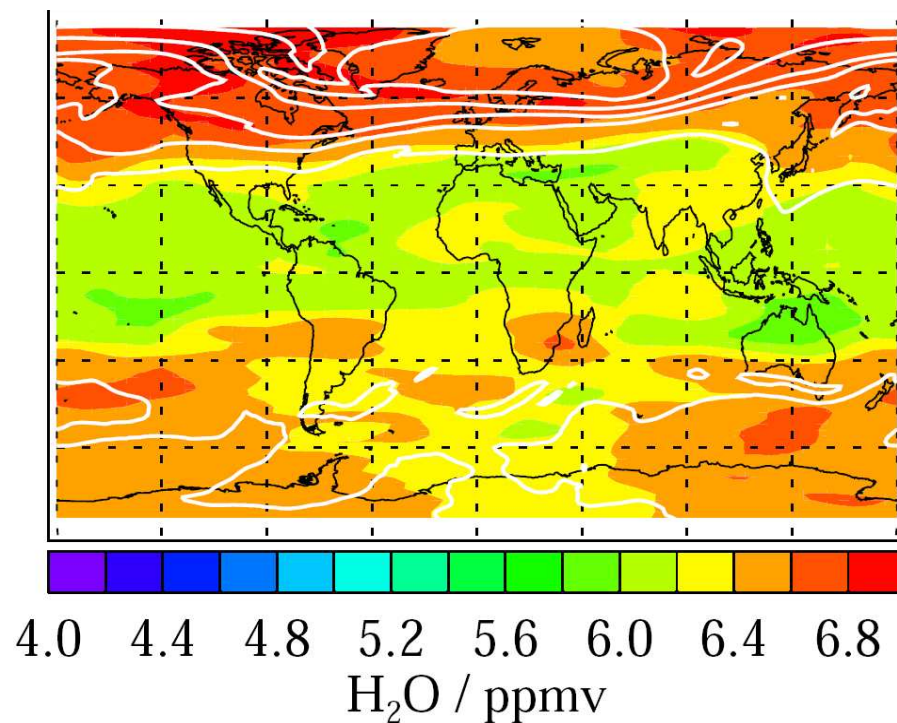


Fig. 10. Aura MLS water vapor at 50 km on 4 November. Air parcels started in the green region near the Carribean islands. Maps available on <http://mls.jpl.nasa.gov/data/gallery.php>.

Title Page

Abstract

Introduction

Conclusions

References

Tables

Figures

◀

▶

◀

▶

Back

Close

Full Screen / Esc

Printer-friendly Version

Interactive Discussion



Water vapor transport in the lower mesosphere

T. Flury et al.

Title Page

Abstract

Introduction

Conclusions

References

Tables

Figures

◀

▶

◀

▶

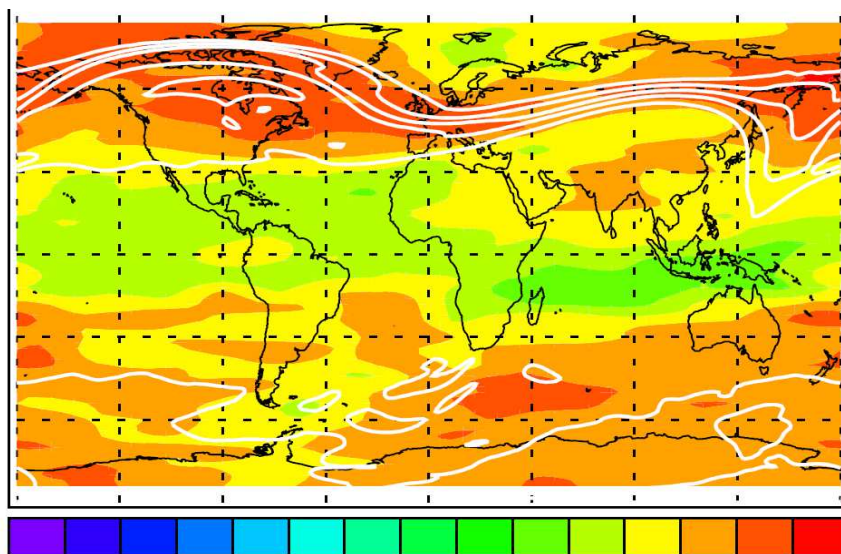
Back

Close

Full Screen / Esc

Printer-friendly Version

Interactive Discussion



4.0 4.4 4.8 5.2 5.6 6.0 6.4 6.8
 $\text{H}_2\text{O} / \text{ppmv}$

Fig. 11. Aura MLS water vapor at 50 km on 8 November. Air parcels started in the orange region over China. Maps available on <http://mls.jpl.nasa.gov/data/gallery.php>.

Water vapor transport in the lower mesosphere

T. Flury et al.

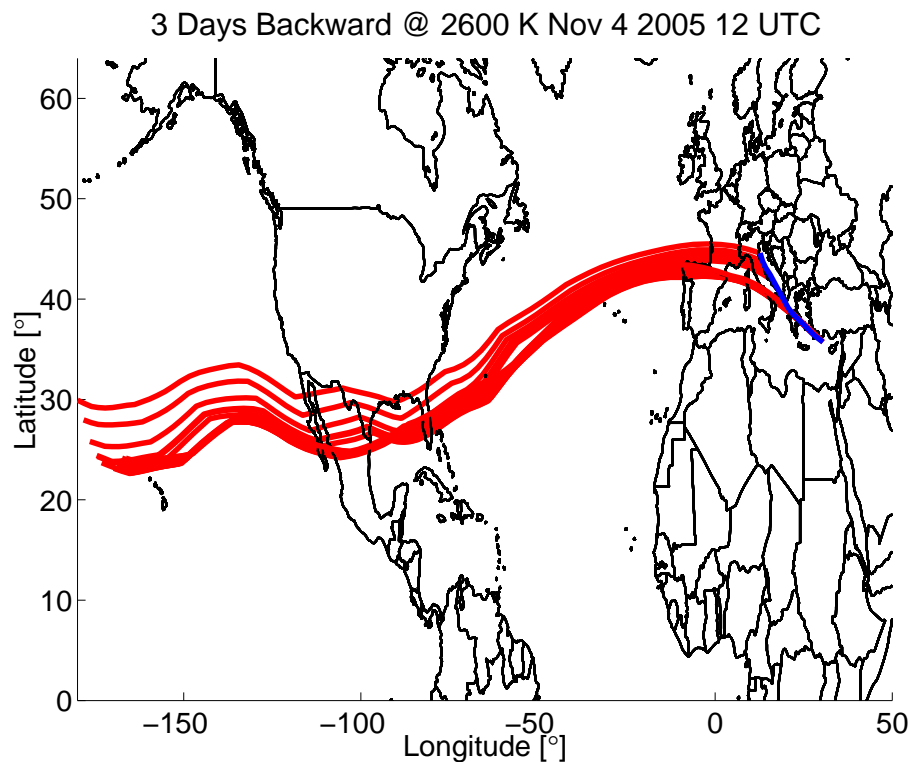


Fig. 12. Backward trajectories along the outward flight conducted on 4 November calculated on the 2600 K isentropes, which is approximately 58 km. The blue line indicates the flight track from north to south. The origin of the air parcels is more south than 12 days later shown in Fig. 13.

Title Page

Abstract

Introduction

Conclusions

References

Tables

Figures

◀

▶

◀

▶

Back

Close

Full Screen / Esc

Printer-friendly Version

Interactive Discussion



Water vapor transport in the lower mesosphere

T. Flury et al.

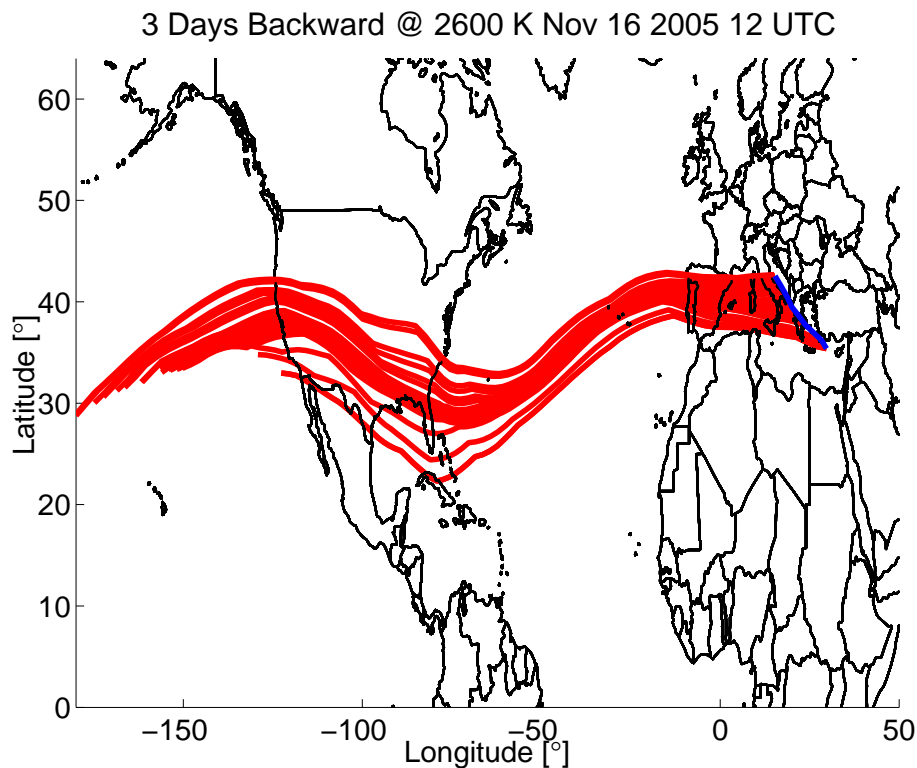


Fig. 13. Backward trajectories along the return flight conducted on 16 November calculated on the 2600 K isentropic. The blue line indicates the flight track south to north. Trajectories pass more north to enter the United States in the beginning than 12 days before as shown on Fig. 9.

Title Page

Abstract

Introduction

Conclusions

References

Tables

Figures

◀

▶

◀

▶

Back

Close

Full Screen / Esc

Printer-friendly Version

Interactive Discussion



**Water vapor
transport in the lower
mesosphere**

T. Flury et al.

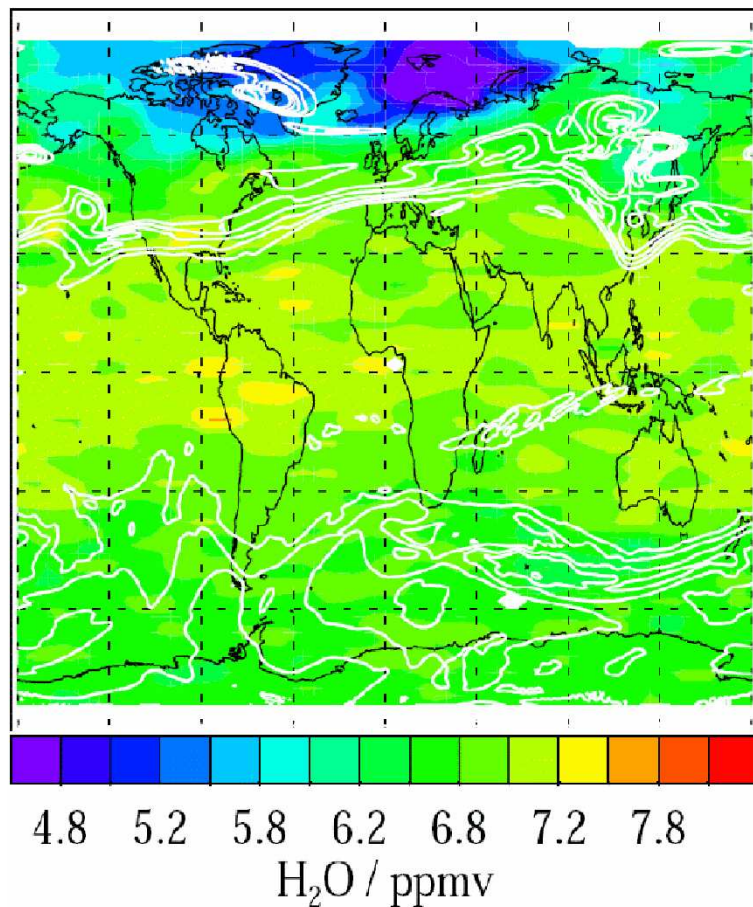


Fig. 14. Aura MLS water vapor at 60 km on 1 November. Air parcels started in the green region of about 6.4 ppm on the west coast of Mexico. Maps available on <http://mls.jpl.nasa.gov/data/gallery.php>.

Title Page

Abstract

Introduction

Conclusions

References

Tables

Figures

◀

▶

◀

▶

Back

Close

Full Screen / Esc

Printer-friendly Version

Interactive Discussion



**Water vapor
transport in the lower
mesosphere**

T. Flury et al.

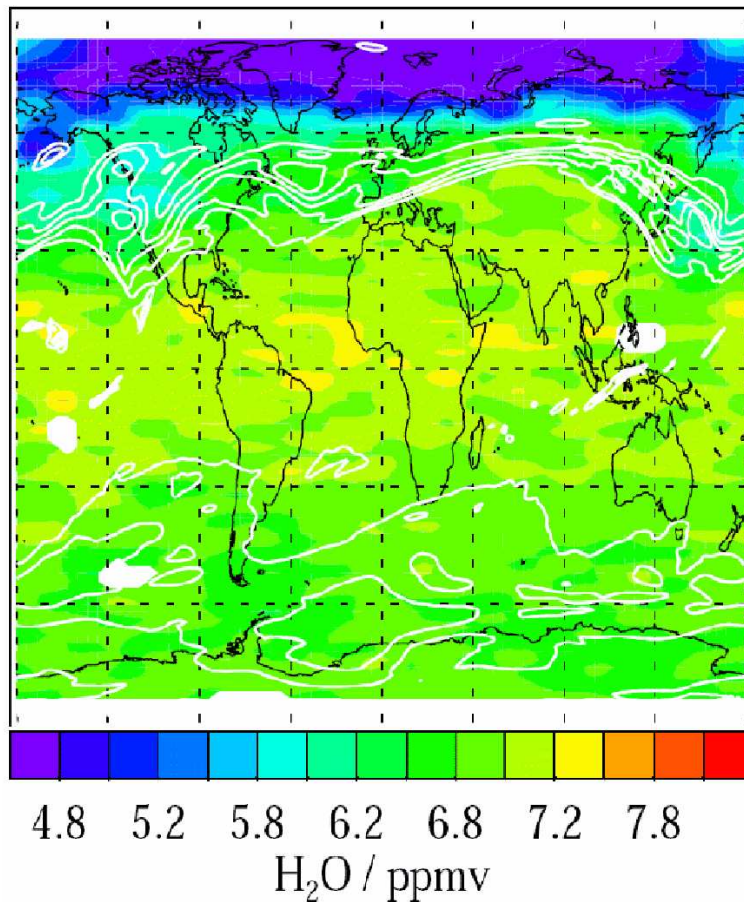


Fig. 15. Aura MLS water vapor at 60 km on 13 November. Air parcels crossed the blue region of about 5.5 ppm on the west coast of the United States. Maps available on <http://mls.jpl.nasa.gov/data/gallery.php>.

Title Page

Abstract

Introduction

Conclusions

References

Tables

Figures

◀

▶

◀

▶

Back

Close

Full Screen / Esc

Printer-friendly Version

Interactive Discussion

